Propagation of elastic waves in one-dimensional periodic stubbed waveguides

Anne-Christine Hladky-Hennion, Christian Granger, and Jérôme Vasseur
Institut d'Electronique de Microélectronique de Nanotechnologie, UMR 8520 CNRS, Avenue Poincaré, Boîte Postale 60069, 59652 Villeneuve d'Ascq Cedex, France

Michel de Billy
Institut Jean Le-Rond d'Alembert, UMR 7190 CNRS, Université Pierre et Marie Curie–Paris 6, 2 Place de la Gare de Ceinture, 78210 Saint-Cyr l'Ecole, France

(Received 27 May 2010; revised manuscript received 5 July 2010; published 29 September 2010)

In this paper, the effect of side branches (or double stub) on the transmission of acoustical wave through periodic structures made of glued beads constituted of solid materials is studied. The displacement picked up at the end of the waveguide is numerically analyzed with the help of the dispersion curves. Experiments are conducted on finite one-dimensional specimens (chains) on which are grafted periodically double stubs. Two situations are investigated in which the mass of the stub beads and beads in the chain are identical or different. The experimental results are compared with numerical calculations and clearly demonstrated that the mechanical properties of the materials are of crucial importance for the width of the pass and forbidden bands (or gaps) as well as the existence of stub, evanescent, and propagating modes.

DOI: 10.1103/PhysRevB.82.104307 PACS number(s): 43.20.+g, 63.20.−e

I. INTRODUCTION

The propagation of waves in periodic media is studied for many years and covers a large area of problems encountered in physics. Due to the existence of allowed and forbidden frequency bands of electromagnetic (e.m.) wave propagation, the so-called photonic crystals (such as modulated dielectric or metallic periodic structure) were investigated in the two last decades both theoretically and experimentally. The studies pointed out that these periodic structures have photonic band gaps (bands of frequencies in which the e.m. waves are forbidden). Many applications of this effect are observed in waves optics with layered structures such as periodic dielectric layers.[1–4] Yablonovitch *et al.*[5] have shown that if the perfect three-dimensional periodicity is broken by a local defect, local e.m. waves can occur within the forbidden band gap. Such periodic systems permit to control the propagation of light and the possibility to build optical devices.

In the last few years, the study of acoustic and elastic wave propagation in periodic materials (known as phononic crystals) has received considerable interest. One of the main reasons for this attention is the rich physics encountered in this kind of wave: the vector character, the mixing of the longitudinal and transverse waves, and the various parameters which control the propagation.

By analogy to photonic materials, several studies have been devoted to the transmission of elastic waves through periodic waveguides (WGs) in one-dimensional (1D) to three-dimensional phononic crystals. The existence of band gaps (frequency range in which no wave is transmitted) in periodic systems was exhibited theoretically and experimentally. Various periodic waveguides were explored: the one-dimensional layered structures,[6,7] the two-dimensional arrays,[5,8–10] and the composite systems[11–19] consisting of liquid or solid circular rods or cavities in epoxy air and water matrix. Other works have reported the band structure and the transmission spectrum for acoustic wave propagation in WG on which periodic side branches of different types are attached periodically: T shape samples,[20–22] double stubs,[23–25] and systems made up of several periodic dangling side branches.[26]

In a recent paper,[27] a study has been performed on the transmission of a short acoustic pulse propagating through chains (or WG) constituted of odd glued metal beads in the middle of which is symmetrically attached a double stub of varying diameter. It has been shown that the frequency of the dip in the response can be adjusted by varying the stub mass, allowing potential applications for the filtering. In the present work, the former study is extended to the case of periodic double stub waveguide made up of spheres glued end to end to realize a finite periodic. The paper presents results on the transmission of elastic wave through a finite number of N identical units (or cells) and show how one can obtain different band structures by varying the properties of the side beads (or stubs) grafted to the main waveguide in a periodic manner.

First, the dispersion curves (wave number versus frequency) and the displacement at the opposite end of the excitation of finite chains times the frequency are numerically calculated. In analogy to photonic crystals, different kinds of resonant structures are observed in the transmission coefficients and are analyzed in terms of stub, evanescent, and propagating modes. Then, an experimental work is devoted to limited specimen including N unit cells. The results show that the acoustic-phonon band structure can be artificially controlled by adjusting the material of the lateral stubs.

II. NUMERICAL ANALYSIS

A. Principle of calculations

Numerical calculations are based on the finite-element method, using the ATILA code.[28] Two types of analysis are performed, considering either infinite or finite periodic chains of beads.

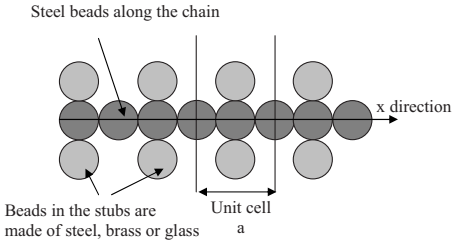

FIG. 1. Sketch of the finite periodic waveguide.

In the case of infinite periodic chains of beads, only one unit cell of the periodic grating is meshed and then Bloch-Floquet relations are applied, which are the phase relations between nodes separated by one spatial period, named a. The calculation, which is a modal analysis,[29] is performed and the dispersion curve is plotted by varying the wave number k in the half Brillouin zone $[0, \pi/a]$. The dispersion curves enable us to deduce propagation modes, cut-off frequencies, and stop bands.[30,31]

In order to study more precisely the transmission through a limited periodic chain of beads with stubs, harmonic analyses are performed at several frequencies. In that case, a prescribed longitudinal force is applied on the left extremity of the chain and the displacements either at the right extremity of the chain or along the stubs, are calculated and displayed. A longitudinal wave is launched on the left side of the phononic crystal. Although mode conversion may occur in the phononic structure, only the longitudinal part of the displacement should be detected on the output side. The numerical variations in the displacement at the end of the chain multiplied by the frequency, noted $U_x f$, are plotted in decibels for a comparison with experimental results. For both determinations, the reference is arbitrary.

To avoid long time of calculation, infinite cylinders are considered instead of beads, using plane strain condition and so a two-dimensional mesh is used, instead of a three-dimensional mesh. Previous numerical tests[27] have shown that this change is valid by using a multiplicative factor on the frequency between the beads and the cylinders results. In the first part of the analysis that is focused on theoretical analysis only, losses are not taken into account. In the second part of the paper, for a better comparison between numerical results and experiments, losses are introduced in the calculation by using complex material constants. In the calculations, the ratio between the imaginary and the real parts of the Young's modulus has been estimated around 1%.[32]

B. Results and analysis: Case of an infinite chain

The results are presented for infinite chains of beads with periodic symmetric stub. The unit cell includes two identical steel beads, 8 mm in diameter. On one of the two beads, two beads are stuck symmetrically. They have the same diameter as the beads along the chain (Fig. 1). The beads along the chain are made up of steel whereas the stub beads are made up of steel, brass, or glass. The mechanical and acoustical properties used in the calculations are presented in Table I. In the study, symmetric stubs have been privileged to avoid bending motions of the whole sample that appear with a nonsymmetric stub. The numerical dispersion curves are given in Figs. 2(a)–2(c) for the stubs made up of steel, brass, and glass, respectively. They are represented as the wave number versus frequency for better further comparisons, but generally, they are classically represented as frequency versus wave number. Vertical lines in our representation correspond to "flat" band in a classical frequency versus wavenumber representation. Therefore, for sake of simplicity, vertical lines are now referred as flat bands. These flat bands have been previously studied in the case of photonic crystals[33] and are related to modes of the stub. The dispersion curves clearly exhibit allowed and forbidden bands. Our investigations are limited to the first five modes. The analysis of Fig. 2 shows three groups of separated branches:

(i) A first group of three branches is observed in the low-frequency part of the dispersion curve. Its width increases

TABLE I. Mechanical and acoustical properties.

Material	E (Young's modulus) (10^{11} N/m)	Poisson's ratio	Density (kg/m^3)	C_L (m/s)	C_T (m/s)
Glass	0.73	0.22	2540	5728	3432
Steel	2.15	0.29	7900	5740	3090
Brass	0.92	0.33	8270	4059	2045

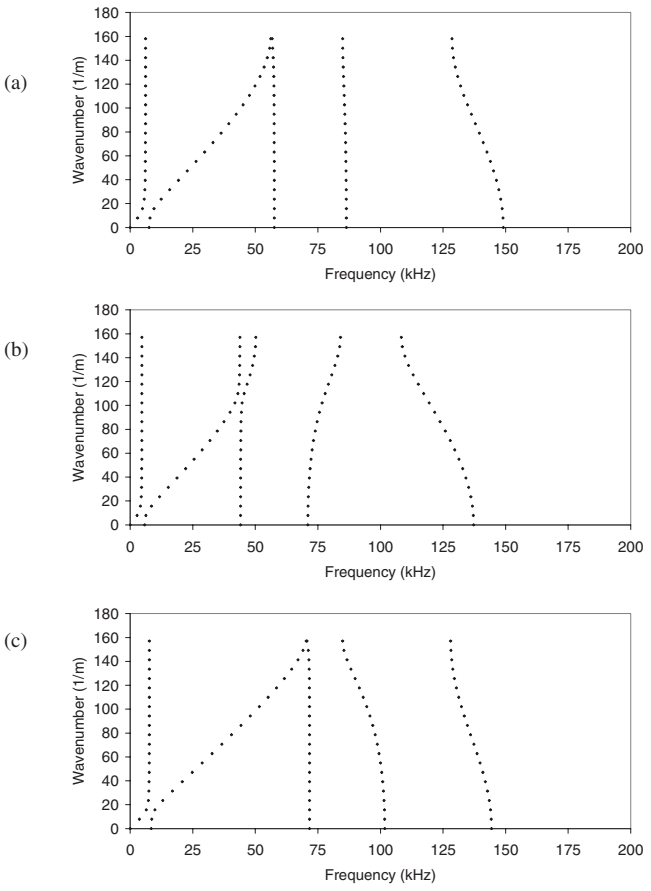

FIG. 2. Dispersion curves (wave number as a function of frequency) with steel beads in the chain and stub made up of (a) steel beads, (b) brass beads, and (c) glass beads.

with the shear velocity of the material which constitutes the stub, named C_T. The first vertical band, which can be referred to a flat band, except for wave number lower than 10 m^{-1}, is related to a bending motion of the stub, later denoted by the letter B. The second band is not vertical. It is dispersive and is related to a propagation mode. Finally, in the case of the particular investigated cells, the last branch of this group appears to be dispersionless mode (or vertical mode) and will be referred also as a flat branch. The mode associated to this branch corresponds to a longitudinal motion of the stub, named stub mode, later denoted by letter S.

(ii) The fourth mode is characteristic of the material in the stub. When the stub beads are the same as the chain beads, this mode is quasidispersionless and the corresponding branch is a vertical line [Fig. 2(a)]. When the stub material is different from the chain material, this mode is transformed into narrow bands as it was previously observed in the case of photonic crystals[33] and exhibits a curvature which may change as it is illustrated in Figs. 2(b) and 2(c). The propagating mode corresponding to this branch will be later denoted by letter F. Additional and systematic numerical calculations have shown that the curvature of the fourth branch seems to change as the ratio between the densities of the beads in the waveguide and in the stubs goes through one. This result is concerned with materials such as glass, brass, steel, aluminum, tungsten, and gold.

(iii) Finally, the fifth branch is a nonvertical band and is related to propagation modes. The curvature of this branch is the same whatever are the materials of the stub and waveguide.

In conclusion, this analysis confirms that the dispersion curves are drastically related to the acoustical and mechanical properties of the materials of stub beads. One can notice that for these periodic specimens, adding stubs of the same material renders the stop bands much larger.

C. Results and analysis: Case of finite chains

In this section, finite chains including $N(1 \leq N \leq 21)$ cells periodically distributed are considered. The displacement component along the chain (U_X) is numerically calculated as a function of the frequency (f) at a detection point situated at the other side of the chain with comparison to the side of the excitation. Then, the variations in the displacement multiplied by frequency $U_X f$ are plotted as a function of the frequency. The resonance phenomena occurring in the 1D phononic crystal made of glued beads can induce different kinds of resonance structures in the transmission coefficients, similar to those depicted in Fig. 8 of Ref. 34. These plots point out a succession of peaks and dips which correspond respectively to maximum and minimum of the displacement in the x direction (main axis of the sample), as previously observed in Ref. 35. Only two of the previous cases are considered (steel stubs and brass stubs), with a view to study the case of a flat band in a band gap and the case of a flat band in a pass band, for various number of cells.

1. Stub beads are made up of steel

In that case, both the beads in the chain and the stub beads are made of steel. Figure 3 presents the frequency variations in $U_X f$ when 6 cells [Fig. 3(b)] and 21 cells [Fig. 3(c)] are considered. The top figure [Fig. 3(a)] is the dispersion curve and allows the identification of the modes. Several observations are done from Figs. 3(b) and 3(c).

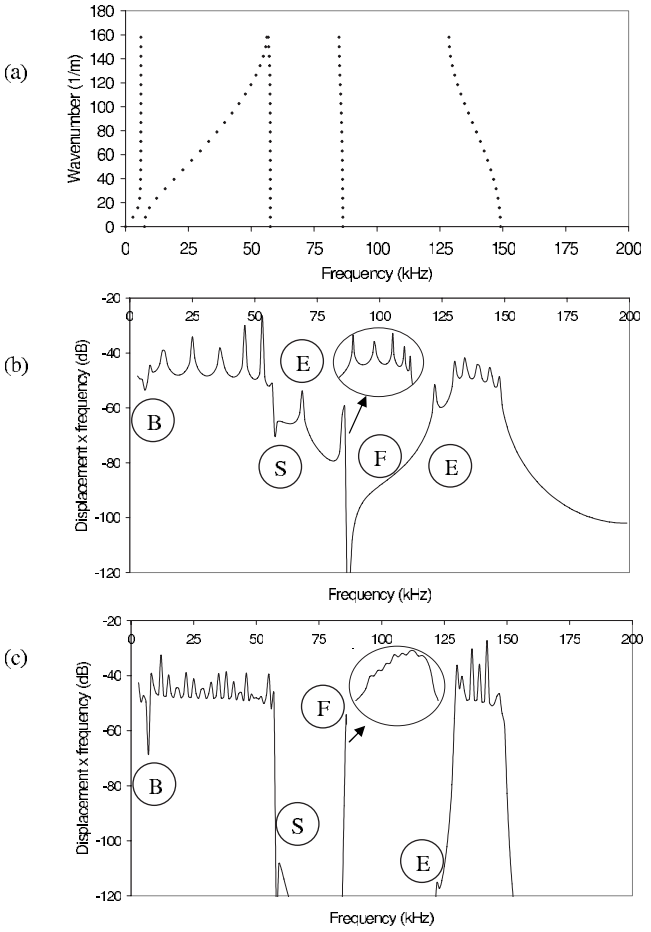

FIG. 3. Steel beads in the chain and in the stubs. (a) Dispersion curve, (b) variations in $U_X f$ as a function of the frequency ($N=6$), and (c) variations in $U_X f$ as a function of the frequency ($N=21$).

(a) In the lower part of the curves, a dip is observed. This dip is associated to a narrow gap which opens up about the crossing point of a flat band and an extended band of propagating modes. It is referred by letter B on the figure. At the frequency for which the dip occurs, the stubs have a bending motion.

(b) Then, the first pass band contains $N-1$ peaks, where N is the number of cells in the waveguide. This has been previously observed in the case of linear chains of beads, without stubs[27] as well as in the case of photonic crystals.[36] These modes are referred as propagation modes, where the displacement along the chain can be written as $\cos(n\pi x/NR)$, with N the number of cells, R the radius of the beads, x the position along the chain, and n an integer ($n=0$ to $N-1$).

(c) The transmission drops drastically at the end of the first group of branches, referred by letter S in Figs. 3(b) and 3(c). This dip is associated to a narrow band gap, as previously observed (see dip B) and corresponds to a longitudinal motion of the stub, referred as a stub mode. The corresponding displacement field is drawn in Fig. 4(a) for $N=6$. One can notice that the main motion is located in the stub: this

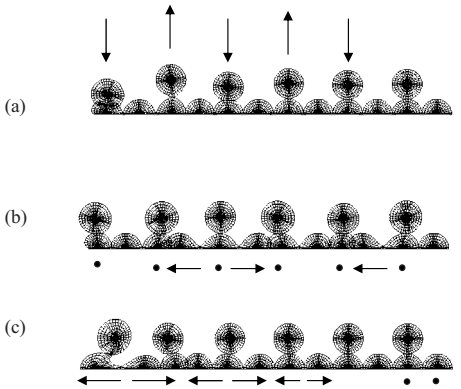

FIG. 4. Steel beads in the chain and in the stubs. $N=6$ cells. Displacement field of different modes (a) stub mode (S), (b) nondispersive flat-band mode (F), and (c) evanescent mode (E). The arrows show the displacement direction whereas the dots correspond to fixed positions.

mode corresponds to a stationary mode of each stub and does not contribute to the transmission.[2]

(d) An isolated peak referred by letter F in Figs. 3(b) and 3(c) appears in the first band gap and is related to the vertical branch (the fourth) in the dispersion curve [Fig. 3(a)]. The inserted figures in Figs. 3(b) and 3(c) are a zoom of the curve in the vicinity of the flat band: it shows a succession of several maxima and minima, which number is related to the number of cells in the waveguide.[36] This "peak" may constitute a "selective filter." Figure 4(b) presents the displacement field of the chain containing six cells at the peak frequency, noticed by letter F in Fig. 3(b): the beads where the stubs are attached do not move whereas the other beads in the chain have a longitudinal motion. This very lightly dispersive mode is referred as a propagating flat-band mode.

(e) In addition, two peaks, referred with letter E in Figs. 3(b) and 3(c) exist in the gaps. The associated modes that do not exist in the dispersion curve correspond to evanescent modes. The peaks are pronounced when the number N is low [Fig. 3(b)] but decrease rapidly as the number of cell increases [Fig. 3(c)]. The corresponding displacement field is presented in Fig. 4(c) for $N=6$, where the evanescent character of the mode is clearly demonstrated.

(f) Finally, the higher pass band contains five peaks, in the case of six cells chain, much more peaks in the case of 21 cells chain but the resolution is not small enough to get the 20 peaks. It corresponds to propagating modes, where $N-1$ peaks are observed when the chain contains N cells.[36]

By varying the number of cells and collecting the values of the resonance frequencies, a numerical spectroscopic diagram is plotted (Fig. 5). This representation, previously used in the case of photonic crystals,[36] shows the spreading of the pass bands, in good accordance with the dispersion curve. It displays several pass bands and gaps in which evanescent modes (E), propagating modes, stub mode (S), bending mode of the stub (B), and flat-band mode (F) can be identified. Notice that for $N=1$, all the modes are observed except the propagating modes and the flat propagating band mode.

2. Stub beads are made up of brass

When the stub beads are made up of brass, Fig. 6 presents the frequency variations in $U_X f$ for 6 [Fig. 6(b)] and 21 cells

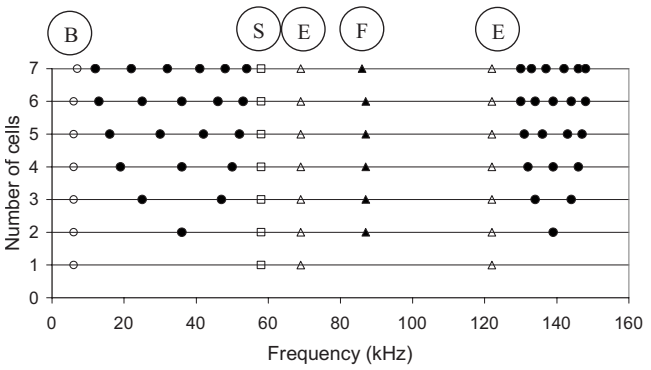

FIG. 5. Steel beads in the chain and in the stubs. Numerical spectroscopic diagram showing the position of the resonance frequencies as a function of the number of cells N ($1 \leq N \leq 7$). Full circles: peaks corresponding to propagating modes in the pass bands, full triangles: peaks related to the (F) band, empty circles: low-frequency dip related to a bending motion of the stub (B), empty triangles: peaks related to evanescent modes (E), empty squares: dip related to a stub mode (S).

[Fig. 6(c)], compared to the dispersion curve [Fig. 6(a)]. The curves are similar to those presented in Fig. 3, except that the mode denoted F (the propagating flat-band mode in the pre-

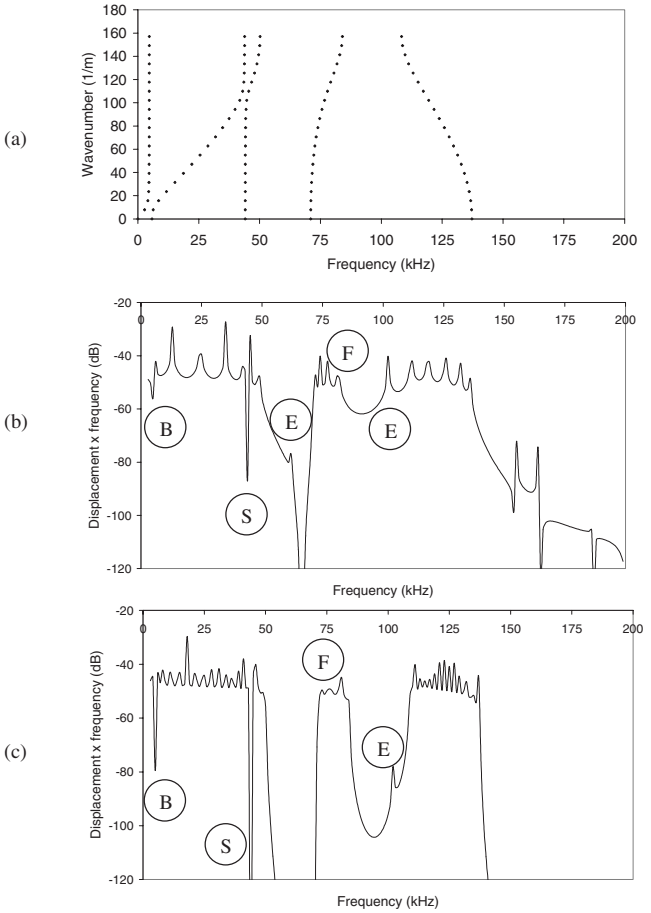

FIG. 6. Steel beads in the chain and brass beads in the stubs. (a) Dispersion curve, (b) variations in $U_X f$ as a function of the frequency ($N=6$), and (c) variations in $U_X f$ as a function of the frequency ($N=21$).

vious case) becomes clearly dispersive. In the same way, the following observations are done: (a) A dip (B) is once again observed in the lower part of the curve, corresponding to the narrow band gap in the dispersion curve, where the stubs have a bending motion. (b) Then, the first pass band contains $N-1$ peaks, related to propagating modes [Fig. 6(b)]. Again the resolution is not small enough to get the 20 peaks [Fig. 6(c)]. (c) A sharp dip is observed near the end of the first pass band, related to a stub mode and referred with letter S in Figs. 6(b) and 6(c). Due to the choice of the materials constituting the chain and the stubs, this mode appears in the pass band. This behavior shows that the sample can be used as a "rejective filter." As the number of cells N is increasing, the depth of the dip is increasing. (d) A narrow pass band appears in the band gap, related to the fourth branch in the dispersion curve, referred with letter F in Figs. 6(b) and 6(c). This time, several peaks are observed directly in the figure, without the need of a precise zoom. This pass band is larger than in the previous case (Fig. 3), due to the particular choice of the beads in the chain and in the stub.[33] Thanks to this pass band, the sample could be used as a selective filter in that case. (e) Once again, evanescent modes are observed, referred with letter E in the figures. They tend to disappear when the number of cells in the sample is increasing. (f) Finally, the last pass band corresponds to propagating modes, containing $N-1$ peaks, where N is the number of cells in the chain.

These calculations confirm the acoustic-phonon band structure and that it is possible to significantly alter it by modifying the material in the stubs. Depending on the nature of the stub, pass band (stop band) could appear in band gap (pass band), inducing a selective (rejective) filter behavior. By an appropriate choice of the periodic stub, one can tailor the acoustic response of the samples.

III. EXPERIMENTAL STUDY

A. Experimental setup and general considerations on experiments

Experiments were conducted on different specimens. Stubs are made by gluing symmetrically and periodically beads on the spheres of the chain. The number (N) of cells in the periodic structure varies from 1 to 6.

A short acoustic pulse is used for the excitation at one of the ends of the chain and the transmitted signal is detected at the opposite side.[37] The power spectrum of the recorded signal is then calculated via a fast Fourier transform and compared to the numerically calculated curves showing the displacement multiplied by the frequency as a function of the frequency.

During experiments, and for a better analysis of the next experimental curves, the following observations have been performed: (a) At very low frequency, a peak—not predicted by the theory—appears in the power spectrum, the resonance frequency of which decreases as the number of cells increases. Additional experiments have confirmed that this mode could be a "chain mode" generated by the contact between the transmitters and the sample and following the Hertz's law.[38] This mode that is probably due to the experimental procedure is pointed out in all the experiments. Therefore, it has been systematically eliminated from the experimental curves as it was done before.[39] (b) The stub modes should appear as a dip in the power spectrum but have not been clearly experimentally identified. (c) The measurements at high frequencies (or low wavelength) may present a large dispersion of the data because the wave is more sensitive to the structure of the contact area between two spheres. This area is not well controlled and can change from one sample to the other. That could produce a dispersion of the data from one record to the other. Therefore, each experimental point corresponds to an average of values over several measurements in different conditions of gluing. For low frequencies, the peak positions of the first branch are not affected by the gluing and the measured dispersion of the data is lower than ± 0.5 kHz. For high frequencies, it can reach ± 2 kHz. (d) At high frequency, attenuation takes place, particularly for the sample with glass stubs.

B. Experimental results

The results presented in this section concern different cases of the unit cell, constituting the investigated waveguide: the chain is always made of steel beads, whereas, the stubs are made of steel, brass, or glass beads. For these samples, the power spectrum are measured and exhibit sharp peaks that correspond to resonance frequencies associated to the different modes generated in the sample.

As an example, Fig. 7 presents two power spectrum experimentally recorded for the samples with brass stubs [Fig. 7(a)] and with glass stubs [Fig. 7(b)], made up of four cells. These records (full lines) are compared with numerical results (dotted lines). Numerical results presented in Sec. II are concerned with cylinders. For a comparison between experimental and numerical results a multiplicative factor on the frequency will be taken into account in the numerical results, as previously explained (cf. Sec. II A). Losses are considered in the materials and estimated around 1%. A reasonably good agreement is observed between the two determinations. The discrepancies which are found between the position of the numerical and the experimental peaks may be due to the modeling that considered cylinders instead of spheres. In the case of brass stubs [Fig. 7(a)], one can notice three regions with peaks ($15<f<45$ kHz, $60<f<70$ kHz, and $85<f<100$ kHz), associated to the two pass bands and the flat pass band (F) [see Fig. 2(b)]. When the stubs are made up of glass [Fig. 7(b)], only the first pass band is observed ($15<f<45$ kHz) in the experimental spectrum, as the attenuation takes place at high frequency. In Figs. 7(a) and 7(b), one can also experimentally and numerically identify other modes such as evanescent mode (E) and propagating flat-band mode (F). The bending (B) and the stub (S) modes are only identified on the numerical curves, and they are detected with difficulty on the experimental spectrum.

Analyses similar to those performed with Fig. 7 are conducted with various lengths of samples (number of cells $1 \leq N \leq 6$). From the power spectrum, the experimental spectroscopic diagrams are built and presented in Figs. 8(a)–8(c) for steel, brass, and glass stubs, respectively. The different

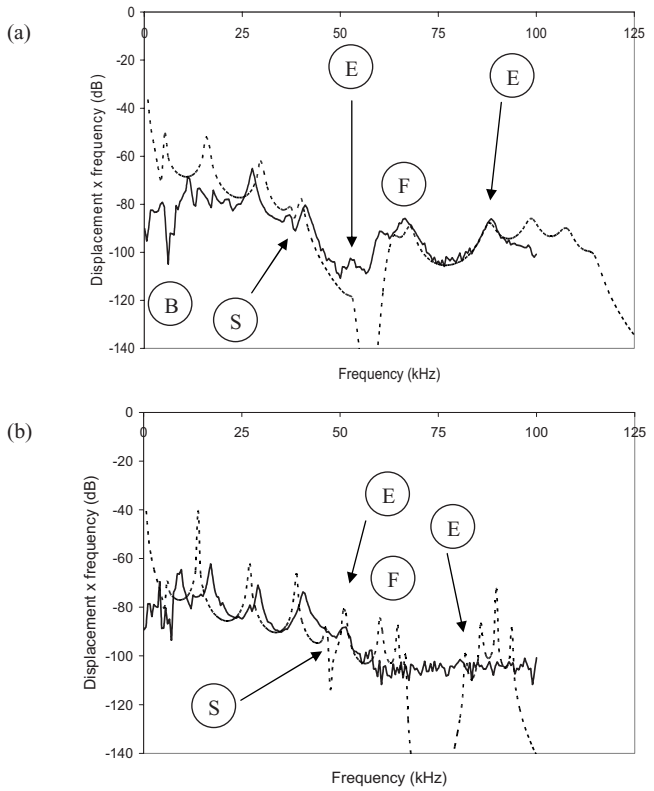

FIG. 7. Numerical displacement multiplied by the frequency (dashed lines) and experimental power spectrum (full lines), versus frequency. (a) Steel beads in the chain and brass beads in the stubs. $N=4$ cells, (b) steel beads in the chain and glass beads in the stubs. $N=4$ cells.

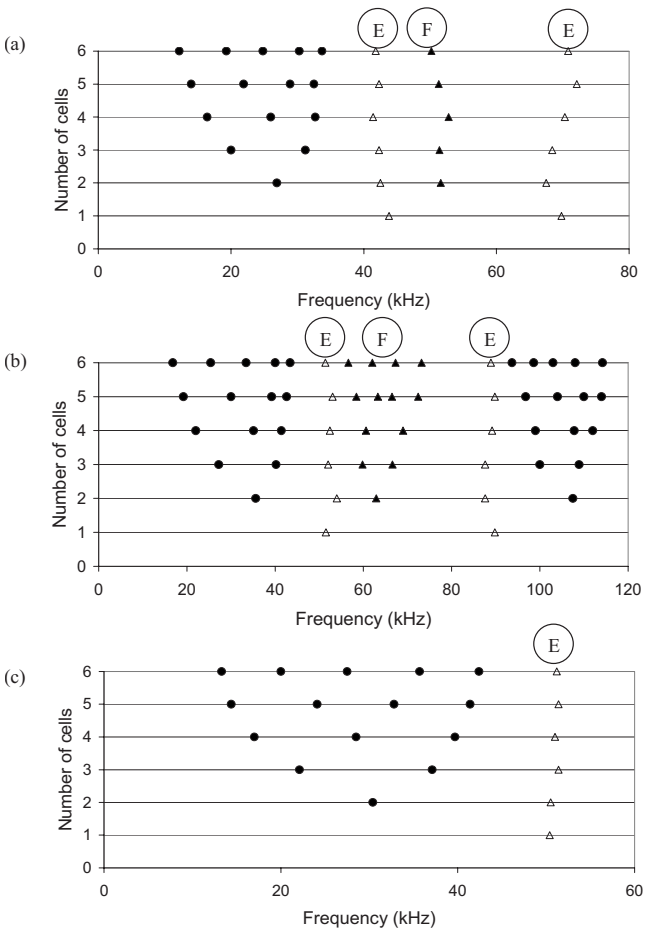

FIG. 8. Experimental spectroscopic diagrams showing the position of the resonance frequencies as a function of the number of cells N ($1 \leq N \leq 6$). (a) Steel beads and steel stubs, (b) steel beads and brass stubs, and (c) steel beads and glass stubs. Full circles: peaks corresponding to propagating modes in the pass bands, full triangles: peaks related to the (F) band, empty triangles: peaks related to evanescent modes (E).

evanescent modes, pass bands, and flat bands are well exhibited. Some of the dots that could be aligned on vertical lines present some small discrepancies: it gives an idea of the accuracy of the measurements. As previously mentioned, the bending (B) and the stub (S) modes are not reproduced on the diagrams because they are not enough marked on the experimental spectrum.

The first spectroscopic diagram [Fig. 8(a)] can be compared easily with the numerical one presented in Fig. 5. One pass band is clearly identified and is related to propagation modes. Then, three modes are identified: the first one and the third one are related to evanescent modes (E) while the second one is associated to a flat propagating mode (F). The frequencies of these three modes are the same whatever the number of cell is.

When the sample has stub beads made up of brass [Fig. 8(b)], three pass bands are identified, similarly to the pass bands observed on the dispersion curves [Fig. 6(a)] and on the previous experimental curve [Fig. 7(a)]. The first and the third pass bands are referred to propagation modes whereas the second one is referred to the dispersive propagating flat band mode (F). Two other modes are observed, which frequencies are independent of the number of cells. Both are identified as evanescent mode (E). Dips corresponding to the stub modes (S) are not clearly identified in the experimental curves.

Finally, when the beads in the chain are made up of steel and the stub beads are made up of glass [Fig. 8(c)], only the low-frequency pass band is identified because attenuation is taking place at higher frequency and no signal is obtained. In addition to the first pass band, an isolated mode is observed at higher frequency: it is an evanescent mode (E).

IV. CONCLUSION

This paper has presented a systematic numerical investigation of the resonance frequencies of a waveguide with grafted periodic double stubs. The present numerical and experimental studies have demonstrated that by a proper choice of the material of the periodic waveguide and stubs, it is possible to optimize the acoustic-phonon band structure. The existence and the properties of gaps, pass bands, and dispersionless modes in the power spectrum of the transmitted acoustical signal through the specimen, are strongly dependent on the material of the stubs with comparison to the one of the waveguide. The presence of stub in the chain intro-

duces dips and peaks in the displacement plots that can have potential applications for rejective and selective filtering. The numerical calculations and the experimental data are qualitatively in good agreement and reproduces well pass band, gaps, evanescent, stub modes, and flat-band modes. This contribution to the propagation of acoustic elastic wave in phononic systems looks to be of a great interest because of the involved physics as it was done in photonic domain. This study has to be extended to the case of cells with different topologies.

ACKNOWLEDGMENT

The authors wish to thank E. H. El Boudouti for fruitful discussions.

[1] J. Carbonell, O. Vanbésien, and D. Lippens, Superlattices Microstruct. **22**, 597 (1997).
[2] K. M. Ho, C. T. Chan, and C. M. Soukoulis, Phys. Rev. Lett. **65**, 3152 (1990); E. Yablonovitch and T. J. Gmitter, *ibid.* **63**, 1950 (1989).
[3] K. M. Leung and Y. F. Liu, Phys. Rev. Lett. **65**, 2646 (1990).
[4] D. Djafari-Rouhani, E. H. El Boudouti, A. Akjouj, L. Dobrzynski, J. O. Vasseur, A. Mir, N. Fettouhi, and J. Zemmouri, Vacuum **63**, 177 (2001).
[5] E. Yablonovitch, T. J. Gmitter, R. D. Meade, A. M. Rappe, K. D. Brommer, and J. D. Joannopoulos, Phys. Rev. Lett. **67**, 3380 (1991).
[6] M. Shen and W. Cao, Appl. Phys. Lett. **75**, 3713 (1999).
[7] M. M. Sigalas and C. M. Soukoulis, Phys. Rev. B **51**, 2780 (1995).
[8] W. M. Robertson and J. F. Rudy, J. Acoust. Soc. Am. **104**, 694 (1998).
[9] M. S. Kushwaha, Appl. Phys. Lett. **70**, 3218 (1997).
[10] M. M. Sigalas, J. Appl. Phys. **84**, 3026 (1998).
[11] M. S. Kushwaha, P. Halevi, L. Dobrzynski, and B. Djafari-Rouhani, Phys. Rev. Lett. **71**, 2022 (1993).
[12] D. Bria and B. Djafari-Rouhani, Phys. Rev. E **66**, 056609 (2002).
[13] Y. Pennec, B. Djafari-Rouhani, J. O. Vasseur, A. Khelif, and P. A. Deymier, Phys. Rev. E **69**, 046608 (2004).
[14] Ph. Lambin, A. Khelif, J. O. Vasseur, L. Dobrzynski, and B. Djafari-Rouhani, Phys. Rev. E **63**, 066605 (2001).
[15] J. O. Vasseur, B. Djafari-Rouhani, L. Dobrzynski, M. S. Kushwaha, and P. Halevi, J. Phys.: Condens. Matter **6**, 8759 (1994).
[16] Z. Hou, X. Fu, and Y. Liu, Phys. Rev. B **70**, 014304 (2004).
[17] M. S. Kushwaha and P. Halevi, Appl. Phys. Lett. **64**, 1085 (1994).
[18] F. R. Montero de Espinosa, E. Jimenez, and M. Torres, Phys. Rev. Lett. **80**, 1208 (1998).
[19] D. García-Pablos, M. Sigalas, F. R. Montero de Espinosa, M. Torres, M. Kafesaki, and N. García, Phys. Rev. Lett. **84**, 4349 (2000).
[20] A. Khelif, B. Djafari-Rouhani, J. O. Vasseur, P. A. Deymier, Ph. Lambin, and L. Dobrzynski, Phys. Rev. B **65**, 174308 (2002).
[21] W. M. Robertson, J. Ash, and J. M. Mc Gaugh, Am. J. Phys. **70**, 689 (2002).
[22] J. Wang, Y. Wang, and H. Guo, Appl. Phys. Lett. **65**, 1793 (1994).
[23] S. Benchabane, A. Khelif, A. Choujaa, B. Djafari-Rouhani, and V. Laude, Europhys. Lett. **71**, 570 (2005).
[24] W. Li and K. Chen, Phys. Lett. A **357**, 378 (2006).
[25] X. F. Wang, M. S. Kushwaha, and P. Vasilopoulos, Phys. Rev. **65**, 035107 (2001).
[26] M. S. Kushwaha, A. Akjouj, B. Djafari-Rouhani, L. Dobrzynski, and J. O. Vasseur, Solid State Commun. **106**, 659 (1998).
[27] A. C. Hladky-Hennion, J. Vasseur, B. Djafari-Rouhani, and M. de Billy, Phys. Rev. B **77**, 104304 (2008).
[28] *ATILA, Version 5.2.1., Finite Element Code for Piezoelectric and Magnetostrictive Transducer Modeling, User's Manual* (ISEN, Acoustics Laboratory, Lille, France, 2002).
[29] Ph. Langlet, A.-C. Hladky-Hennion, and J.-N. Decarpigny, J. Acoust. Soc. Am. **98**, 2792 (1995).
[30] L. Brillouin, *Wave Propagation in Periodic Structures* (Dover, New York, 1953).
[31] C. Kittel, *Introduction to Solid State Physics* (Wiley, New York, 1996).
[32] R. Holland, IEEE Trans. Sonics Ultrason. **SU–14**, 18 (1967).
[33] B. Djafari-Rouhani, E. H. El Boudouti, A. Akjouj, J. O. Vasseur, and L. Dobrzynski, Prog. Surf. Sci. **74**, 389 (2003).
[34] G. Gantzounis and N. Stefanou, Phys. Rev. B **72**, 075107 (2005).
[35] R. Sainidou, N. Stefanou, I. E. Psarobas, and A. Modinos, Z. Kristallogr. **220**, 848 (2005).
[36] E. H. El Boudouti, Y. El Hassouani, B. Djafari-Rouhani, and H. Aynaou, Phys. Rev. E **76**, 026607 (2007).
[37] M. de Billy, J. Acoust. Soc. Am. **108**, 1486 (2000).
[38] L. D. Landau and E. M. Lifshitz, *Theory of Elasticity* (Pergamon Press, Oxford, 1986).
[39] A. C. Hladky-Hennion and M. de Billy, J. Acoust. Soc. Am. **122**, 2594 (2007).